



Quantifying the range of future glacier mass change projections caused by differences among observed past-climate datasets

Megumi Watanabe^{1,2} · Aki Yanagawa³ · Satoshi Watanabe⁴ · Yukiko Hirabayashi⁵ · Shinjiro Kanae¹

Received: 30 August 2018 / Accepted: 18 June 2019 / Published online: 26 June 2019
© The Author(s) 2019

Abstract

Observed past climate data used as input in glacier models are expected to differ among datasets, particularly those for precipitation at high elevations. Differences among observed past climate datasets have not yet been described as a cause of uncertainty in projections of future changes in glacier mass, although uncertainty caused by varying future climate projections among general circulation models (GCMs) has often been discussed. Differences among observed past climate datasets are expected to propagate as uncertainty in future changes in glacier mass due to bias correction of GCMs and calibration of glacier models. We project ensemble future changes in the mass of glaciers in Asia through the year 2100 using a glacier model. A set of 18 combinations of inputs, including two observed past air temperature datasets, three observed past precipitation datasets, and future air temperature and precipitation projections from three GCMs were used. The uncertainty in projected changes in glacier mass was partitioned into three distinct sources: GCM uncertainty, observed past air temperature uncertainty, and observed past-precipitation uncertainty. Our findings indicate that, in addition to the differences in climate projections among GCMs, differences among observed past climate datasets propagate fractional uncertainties of about 15% into projected changes in glacier mass. The fractional uncertainty associated with observed past precipitation was 33–50% that of the observed air temperature. Differences in observed past air temperatures and precipitation did not propagate equally into the ultimate uncertainty of glacier mass projection when ablation was dominant.

Keywords Propagation of uncertainty · Glacier model · Bias correction · Calibration · Air temperature · Precipitation

Electronic supplementary material The online version of this article (<https://doi.org/10.1007/s00382-019-04868-0>) contains supplementary material, which is available to authorized users.

✉ Megumi Watanabe
megumi@rainbow.iis.u-tokyo.ac.jp

- ¹ Department of Civil and Environmental Engineering, Tokyo Institute of Technology, 2-12-1, O-okayama, Meguro-ku, Tokyo 152-8552, Japan
- ² Institute of Industrial Science, The University of Tokyo, 4-6-1, Komaba, Meguro-ku, Tokyo 153-8505, Japan
- ³ School of Science and Engineering, Meisei University, 2-1-1 Hodokubo, Hino, Tokyo 191-8506, Japan
- ⁴ School of Engineering, The University of Tokyo, 7-3-1 Hongo, Bunkyo-ku, Tokyo 113-8656, Japan
- ⁵ Department of Civil Engineering, Shibaura Institute of Technology, 3-7-5 Toyosu, Koto-ku, Tokyo 135-8548, Japan

1 Introduction

Worldwide, glaciers have reacted sensitively to recent changes in climate forcing and are expected to experience continued mass loss throughout the twenty-first century (Stocker 2014). Glacial retreat raises major concerns about the sustainability of global and local water resources, sea level rise, and natural hazards (Immerzeel et al. 2010; Kaser et al. 2010; Fujita et al. 2013; Stocker 2014). Future global mass changes in glaciers are predicted by various glacier models. Several studies have attempted to predict future changes worldwide (Marzeion et al. 2012; Hirabayashi et al. 2013; Radić et al. 2014; Huss and Hock 2015). To simulate such changes, glacier models use climate projections as input such as future air temperature and precipitation from general circulation models (GCMs). The climate projections of the various GCMs differ markedly, even among those using the same emissions scenarios (Stocker 2014). Such ranges are defined as “uncertainties” in the present study. Uncertainty in terms of climate prediction has

several distinct sources. Model uncertainty reflects limitations in model structure and the parameterization used to represent geophysical processes. The internal variability of a climate system reflects the natural fluctuations that arise in the absence of any radiative forcing of the planet. These model uncertainties and internal variabilities will here be termed “GCM uncertainties.” We used a single climate scenario (RCP8.5); we did not explore scenario uncertainty. Uncertainties among climate projections propagate to projections of mass changes along the modeling chain, thus from GCMs to glacier models. The latter models address these uncertainties when projecting future changes in glacier mass (Marzeion et al. 2012; Hirabayashi et al. 2013; Radić et al. 2014; Huss and Hock 2015).

The range of future climate projections among GCMs is not the only source of uncertainty in projections of future changes in glacier mass. Even observed past air temperatures and precipitation, which are used as input data in glacier models, are expected to differ among climate datasets. These differences could also cause uncertainty in projections. The differences among climate datasets arise from spatiotemporal interpolation of naturally discontinuous and intermittent field data and the assumptions needed to obtain physical measurements from remote sensing (Global Energy and Water Exchanges 2013).

As is well known, the significant differences among observed past precipitation datasets derived from mountainous areas reflect under-representation of gauge locations at high elevations and wind-induced undercatch of solid precipitation (Adam et al. 2006; Hirabayashi et al. 2008a; Bismans et al. 2009). Some authors have expressed concern that these differences might affect simulations of glacio-hydrological budgets (Bookhagen and Strecker 2008; Andermann et al. 2011; Palazzi et al. 2012; Dahri et al. 2016). The differences may markedly influence projections of future changes in glacier mass.

Differences among past air temperature and precipitation datasets propagate uncertainties into simulations featuring bias correction of GCMs, and calibration (Fig. 1); both of these steps are required when projecting changes in glacier mass using glacier models (Marzeion et al. 2012; Hirabayashi et al. 2013; Radić et al. 2014; Huss and Hock 2015). The data serve as references for bias correction and forcing factors when calibrating glacier models that seek to determine parameters such as melting factors and adjustment parameters for climatic data. Thus, uncertainties in climatic datasets propagate into projections of future changes in glacier mass.

Most previous glacier model studies have used a single air temperature dataset and a single precipitation dataset to project changes in glacier mass, and did not assess the uncertainty arising from differences among climate datasets (Marzeion et al. 2012; Giesen and Oerlemans 2013;

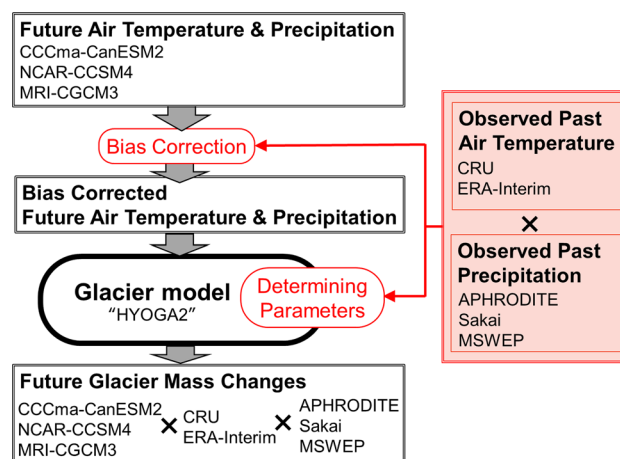


Fig. 1 Overview of projection of changes in glacier mass. “Future Air Temperature & Precipitation” data from the climate projections of GCMs (CCCma-CanESM2, NCAR-CCSM4, and MRI-CGCM3) served as climate forcing factors when making predictions. The “Future Air Temperature & Precipitation” data were corrected by the “Bias Correction” procedure using “Observed Past Air Temperature” (CRU, ERA-Interim) and “Observed Past Precipitation” (APHRODITE, Sakai, MSWEP) as references. The “Observed Past Air Temperature” and the “Observed Past Precipitation” also served as forcing factors in the “Glacier model HYOGA2” during calibration of “Determining Parameters.” Finally, using “Bias Corrected Future Air Temperature & Precipitation” as a future climate forcing parameter, the “Glacier model HYOGA2” calculated “Future Glacier Mass Changes” for each combination of input data (18 combinations of three “Future Air Temperature & Precipitation” datasets of the GCMs, two “Observed Past Air Temperature” datasets, and three “Observed Past Precipitation” datasets). Here, “X” indicates combinations

Hirabayashi et al. 2013; Bliss et al. 2014; Huss and Hock 2015). Why this is so is unknown but studies using other impact models such as hydrological models have also tended to do this. One reason could be that it is difficult to handle heterogeneous climate datasets with different spatiotemporal resolutions, domains, and data formats, and this hampers assessment of the impacts of uncertainty derived from those datasets.

Koppes et al. (2015) assessed the temperature-sensitivity of glacier meltwater to 2100 in terms of observed past air temperature data; past climate forcing in the Indus River basin was evaluated. The glacier model parameters were constant among all simulations, even when different observed past air temperatures were employed; GCMs were not used to project future changes in glacier mass. Thus, a further study assessing the impacts of differences among observed past air temperatures and precipitation is necessary. In addition, the uncertainties propagated by bias correction of GCMs and determination of glacier model parameters require evaluation because most prior glacier models used such methods.

The HMA contains the largest mass of land glacier ice with the exception of the poles. The HMA glaciers are retreating and losing mass at rates comparable to glaciers in other regions of the world (Fujita and Nuimura 2011; Bolch et al. 2012; Kääb et al. 2012; Brun et al. 2017). Meltwaters from HMA glaciers flow into downstream rivers; large human populations depend on glacier-fed water supplies. The impact of climate change on the extent of glacier melt is of major interest. The HMA includes the Tibetan Plateau, for which observed climatic datasets and GCM climate projections are among the sparsest worldwide (Stocker 2014). This region is characterized by high-level orography and a large proportion of solid precipitation, both of which would be expected to greatly bias observations.

Therefore, we assessed the uncertainty caused by differences in observed past air temperature and precipitation datasets, and also uncertainty arising from differences among GCMs. The uncertainties in future glacier mass change projections caused by the differences in observed past climate data used to correct GCM biases and calibrate glacier models were assessed. We focused on particularly the HMA, for which past air temperature and precipitation data are scant and GCM future climate projections are uncertain.

2 Methods

2.1 Overview

We projected changes in the mass of Asian glaciers through 2100 using a glacier model based on two observed past air temperature datasets, three observed past precipitation datasets, and three GCMs to quantify the potential uncertainties, as described above (Fig. 1). The uncertainty was partitioned into three distinct sources: GCM uncertainty, observed past air temperature uncertainty, and observed past precipitation uncertainty.

2.2 Targeted glaciers

Our study region was the high mountains of Asia (26.5–55.5N, 66.5–104.5E), corresponding to central, southwestern, and southeastern Asia, as well as the Altay and Sayan regions of northern Asia in the Randolph Glacier Inventory (RGI6.0). In this area, 19 observations of glacier mass balance are available for use in calibrating glacier models for experiments. Eight of these data points were well calibrated (i.e., calibration errors were within $\pm 50\%$). Some points were not well calibrated: warm bias was evident in observed air temperature datasets, the observed precipitation datasets exhibited large spreads, and the quality of mass balance observations was suspect. From 1084 glaciers located near the eight points in the RGI6.0, 28 glaciers where the

range of mass balance for the calibration period was small in all simulation runs were chosen randomly (reliability: 95%; request error: 5%). The area-weighted means of the mass balances of these 28 glaciers shown in Fig. 2 were used to assess uncertainty in the experiments.

2.3 Glacier model

We used the model HYOGA2, which was developed for global-scale mass-balance calculations and applied to project the volume evolution of all glaciers outside the Antarctic and Greenland ice sheets through 2100 (Hirabayashi et al. 2013). We updated the calibration method for the glacier model to quantify each source of uncertainty in the mass change projections of Asian glaciers (see 2.5.2. for details; Watanabe et al. 2018). The distributed glacier input data for the model was also updated to the latest RGI.

Glacier mass balance was calculated using the glacier model forced by daily precipitation and surface air temperature. The melt rates of the surfaces of snow and ice at each elevation band were calculated using a simple degree-day approach and then aggregated to estimate the mass balance for each glacier. Subgrid-scale variation in changes in glacier and snow mass was considered by dividing a model grid cell into 50 m elevation bands. The surface air temperature was assumed to decrease at a constant lapse rate of $-0.65\text{ }^{\circ}\text{C}$ (100 m^{-1}). We did not incorporate precipitation lapse rates because each precipitation dataset considered the orography. We calculated the differences between the grid cell altitudes of each observed air temperature dataset and the median glacier altitude. We used this difference to derive the temperature lapse rate for each glacier. The model assumes that only snow affects the mass balance. Precipitation was assumed to be snow if the air temperature of the elevation band was less than or equal to $2\text{ }^{\circ}\text{C}$. The basic model structure is similar to that of other global glacier models such as the Global Glacier Evolution Model (GloGEM; Huss and Hock 2015), the

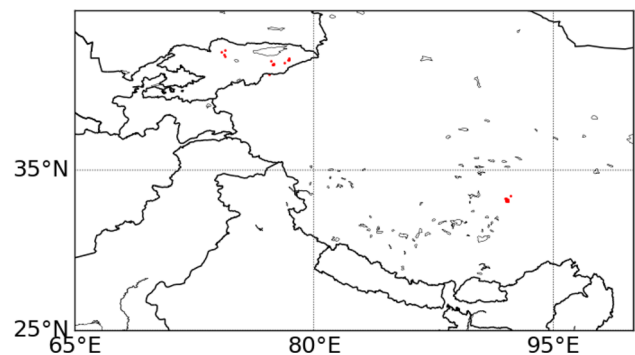


Fig. 2 Location of targeted glaciers (26.5–55.5N, 66.5–104.5E). Red dots show the centers of each targeted glacier. Black lines: Geopolitical borders

Radic and Hock model (Radić et al. 2014), and the Marzeion model (Marzeion et al. 2012).

In our study area, the average annual mass balance of the 28 HMA glaciers (Sect. 2.2 and Fig. 2) was simulated as -0.21 ± 0.14 m w.e. year⁻¹ from 2003 to 2009. The observed annual mass balance of all HMA glaciers was -0.22 ± 0.10 m w.e. year⁻¹ from 2003 to 2009 (Gardner et al. 2013). The modeled and observed values are similar, although a direct comparison is inappropriate. The root mean-square error between the modeled and observed mass balances (Gardner et al. 2013) was 0.14 m w.e. year⁻¹, thus less than the error range of other global glacier models (Marzeion et al. 2012; Radić et al. 2014), although, again, direct comparisons are inappropriate. Marzeion et al. (2012) reported that the root mean error between the modeled and observed mass balance of HMA (North) was 0.33 ± 0.11 m w.e. year⁻¹; for HMA (West) 0.42 ± 0.20 m w.e. year⁻¹; and for HMA (South) 0.37 ± 0.16 m w.e. year⁻¹. Radić et al. (2014) reported that the root mean error between the modeled and observed HMA mass balance was 1.05 m w.e. year⁻¹. The latest model study (Huss and Hock 2015) estimates were -0.05 m w.e. year⁻¹ for 2001–2005 and -0.3 m w.e. year⁻¹ for 2006–2010 for the HMA. Our results are similar (-0.02 m w.e. year⁻¹ for 2001–2005; -0.36 m w.e. year⁻¹ for 2006–2010).

2.4 Observed past air temperature and precipitation data

Observed past air temperature and precipitation datasets were used as references for bias correction of GCMs and calibration of the glacier model to determine parameters. To evaluate the uncertainty in projections of changes in glacier mass arising from the observed past climate datasets, a set of six combinations of two observed past air temperature datasets and three observed past precipitation datasets was defined. We used CRU air temperature, ERA-Interim air temperature, APHRODITE precipitation, Sakai precipitation, and MSWEP precipitation. These six combinations met the following conditions: temporal resolution, daily; spatial resolution, $\leq 0.5^\circ$; and period, from 1980. We were also influenced by earlier glacier model studies. The differences among the selected observed past

Table 1 Climate forcing used for GCM calibration and bias correction

Used data	Temperature (°C)
CRU	- 7.8
ERA-Interim	- 8.8

Annual average air temperatures for 1980–2004 in the targeted glacierized areas

air temperature and precipitation datasets were described in Tables 1, 2 and 3.

CRU provides gridded surface air temperature and precipitation data; CRU TS 3.10 interpolates in situ observations and has often been used in global glacier modeling studies (Marzeion et al. 2012, 2018; Giesen and Oerlemans 2013; Hirabayashi et al. 2013; Slangen et al. 2017). In terms of gridded precipitation data based on in situ observations in Asia, the precipitation product suite “Asian Precipitation-Highly Resolved Observational Data Integration Towards Evaluation of Water Resources” (APHRODITE; Yatagai et al. 2012) features the most extensive rain gauge network and has been used to project mass changes in Asian glaciers in preference to global precipitation datasets such as that of the CRU (Lutz et al. 2014). Hence, we used a combination of CRU-based temperature (Hirabayashi et al. 2008b) and APHRODITE-based precipitation data.

Some glacier models use re-analyses of climate data, such as the air temperature and precipitation data from ERA-40, ERA-Interim, or WDEFI that were originally provided by the European Centre for Medium-Range Weather Forecasts (ECMWF), to project changes in glacier mass. Such models typically produce less accurate estimates of precipitation than of air temperature (Parker 2016). Precipitation re-analyses often require further downscaling, particularly for high-elevation sites (Radić et al. 2014). Radić et al. (2014) used ECMWF reanalysis data for air temperature and another gridded precipitation product based on interpolated in situ observations (Beck et al. 2005).

Moreover, gridded precipitation products that interpolate in situ observations, including APHRODITE, often underestimate precipitation at high elevations (Adam et al. 2006; Sakai et al. 2015). To overcome this issue, Sakai and Fujita (2017) used a combination of ECMWF reanalysis

Table 2 Climate forcing used for GCM calibration and bias correction

Used data	Precipitation (mm year ⁻¹)
APHRODITE	378
Sakai	566
MSWEP	714

Annual total precipitation for 1980–2004 in the targeted glacierized areas

Table 3 Coefficients of variation in annual average air temperatures and annual total precipitation among datasets used for GCM calibration and bias correction, 1980–2004 in the targeted glacierized areas

Variable	CV
Air temperature	- 0.06
Precipitation	0.25

air temperature and APHRODITE data corrected based on regional-scale analyses of glacier morphometry (Sakai et al. 2015; ‘Sakai precipitation’) to calculate changes in the mass of glaciers in Asia. Beck et al. (2017) corrected precipitation observations using gauged discharge data when developing Multi-Source Weighted-Ensemble Precipitation (MSWEP), the latest global gridded precipitation product. In this study, we combined ECMWF reanalyses of air temperature and MSWEP gridded precipitation to project future changes in glacier mass.

Furthermore, we used three other combinations of air temperature and precipitation datasets (CRU temperature–Sakai precipitation, CRU temperature–MSWEP precipitation, ERA-Interim temperature–APHRODITE precipitation) to assess the uncertainty in projections of future changes in glacier mass arising from the observed past air temperature and precipitation datasets.

2.5 Climate forcing for future predictions

Simulations of future glacier mass balance were forced by three GCMs (CCCma-CanESM2, NCAR-CCSM4, MRI-CGCM3) involved in the fifth phase of the Coupled Model Inter-comparison Project (CMIP5) using the highest emissions scenario (representative concentration pathway [RCP] 8.5). Three GCMs were selected to cover the range of future changes in glacier mass based on a preliminary experiment for glaciers in the HMA (Supplement 1). Glacier melt in the twenty-first century was projected from the preliminary experiment using nine GCMs, which were selected based on the availability of variables for input to the glacier model (HYOGA2) and to avoid duplication of GCM developers. Among the nine GCMs, CCCma-CanESM2, NCAR-CCSM4, and MRI-CGCM3 projected the greatest, median, and smallest changes in glacier mass, respectively. The differences of future air temperature and precipitation among the selected three GCMs were described in Tables 4, 5 and 6.

Table 4 Climate forcing for future projections

Used data	Temperature (°C)
CCCma-CanESM2	−2.9
NCAR-CCSM4	−4.0
MRI-CGCM3	−4.5

Annual average air temperatures from the GCMs (bias corrected using ERA-Interim, before the application of the adjustment factor dT) for 2060–2080 in the targeted glacierized areas

Table 5 Climate forcing for future projections

Used data	Precipitation (mm year ^{−1})
CCCma-CanESM2	796
NCAR-CCSM4	699
MRI-CGCM3	896

Annual total precipitation from the GCMs (bias corrected using MSWEP, before the application of the adjustment factor C_p) for 2060–2080 in the targeted glacierized areas

2.6 Bias correction

Despite continuous efforts to improve the capability of GCMs to simulate historical climates, the use of downscaling methods is essential for impact assessment studies of climate change. In this study, a statistical downscaling method called “bias correction” was applied to GCM-simulated data because it has a lower computational cost than dynamical downscaling approaches. We used a trend-preserving bias-correction method (Watanabe et al. 2012) to preserve GCM-simulated signals in future projections. This rendered it possible to assess uncertainties in glacier projection induced by variation among GCMs. We used two observed past air temperature and three observed past precipitation datasets as reference data when bias-correcting three GCMs. The GCM simulation data were compared to observation-based daily climatic data to estimate biases over the 30 years from 1981 to 2010 (1981 to 2007 for the APHRODITE and Sakai precipitations). During bias correction, we adjusted means, temperature standard deviations, and precipitation coefficients of variance. Finally, the GCM-simulated daily air temperature and precipitation data for 2006–2100 were corrected.

2.7 Glacier model parameters

We derived model parameters via calibration. Hirabayashi et al. (2013) calibrated the degree-day factors (DDFs) for ice and snow with HYOGA2. We calibrated the adjustment factors for precipitation (C_p) and temperature (dT) data in addition to the DDFs with HYOGA2, as have previous studies (Marzeion et al. 2012; Radić et al. 2014; Huss and Hock 2015). The calibration order was that of Huss and Hock (2015). Individual glacier data obtained from the RGI were first aggregated into a large glacier per 0.5° grid cell. Then the parameters for each

Table 6 Coefficients of variation in annual average air temperatures and annual total precipitation among the bias corrected GCMs, 2060–2080 in the targeted glacierized areas

Variable	CV
Future air temperature	−0.17
Future precipitation	0.10

cell were calibrated until we obtained the maximum extent of agreement with the cell-specific long-term (1981–2004) average of the total glacier mass balance. The gridded mass balance data of Hirabayashi et al. (2013), which are based on those of others (Dyurgerov and Meier 1997, 2005; Serreze et al. 2000; Dyurgerov 2010), were used for calibration. Each parameter was determined for each of six combinations of observed past air temperature and precipitation data (Table 7). We did not calibrate the Sakai precipitation because the data are already calibrated (Sakai et al. 2015).

2.8 Sources of uncertainty

As mentioned above, we partitioned uncertainty into GCM, observed past air temperature, and observed past precipitation uncertainties following Hawkins and Sutton (2011) and Wada et al. (2013). We calculated the variance of each uncertainty, assuming that they were independent. The total variance (V_t) was the sum of the variance of climate projections from the GCMs (V_g), the variance among different observed past air temperature datasets (V_a), and the variance among different observed past precipitation datasets (V_p). V_g was approximated by calculating the variance across the GCMs for a given observed past air temperature and precipitation dataset pair, repeating this exercise for each dataset combination, and then calculating an average variance. V_a and V_p were calculated in the same manner. We preferred this method because the works of both Hawkins and Sutton (2011) and Wada et al. (2013)

Table 7 Simulation settings used to project future changes in glacier mass using two observed past air temperature datasets, three observed past precipitation datasets and future air temperature and precipitation data yielded by three GCMs

	Obs. past T	Obs. past P	GCM (future T and P)
1	CRU	APHRODITE	CCCma-CanESM2
2	CRU	APHRODITE	NCAR-CCSM4
3	CRU	APHRODITE	MRI-CGCM3
4	ERA-Interim	APHRODITE	CCCma-CanESM2
5	ERA-Interim	APHRODITE	NCAR-CCSM4
6	ERA-Interim	APHRODITE	MRI-CGCM3
7	CRU	Sakai	CCCma-CanESM2
8	CRU	Sakai	NCAR-CCSM4
9	CRU	Sakai	MRI-CGCM3
10	ERA-Interim	Sakai	CCCma-CanESM2
11	ERA-Interim	Sakai	NCAR-CCSM4
12	ERA-Interim	Sakai	MRI-CGCM3
13	CRU	MSWEP	CCCma-CanESM2
14	CRU	MSWEP	NCAR-CCSM4
15	CRU	MSWEP	MRI-CGCM3
16	ERA-Interim	MSWEP	CCCma-CanESM2
17	ERA-Interim	MSWEP	NCAR-CCSM4
18	ERA-Interim	MSWEP	MRI-CGCM3

were similar to ours, in that three or four climate scenarios and 5 to 14 GCMs were used to assess fractional uncertainties.

3 Results

3.1 Projected annual mass balance of glaciers

The model projected a total of 18 mass change patterns in Asian glaciers through 2100 using two observed past air temperature datasets, three observed past precipitation datasets, and three GCMs (Table 8, Fig. 3). All simulations projected continuous mass loss throughout the twenty-first century (Fig. 3). The magnitude of loss varied substantially depending on the extent of the temperature increase and associated precipitation changes, which were determined by the choice of air temperature and precipitation products as well as the GCM. The average annual mass loss was projected to be around -3 m w.e. year⁻¹ by the end of the twenty-first century. The projection range was from around -2 m w.e. year⁻¹ to a maximum of almost -5 m w.e. year⁻¹.

3.2 Attribution of uncertainties in projected changes in glacier mass

Figure 4 shows the fraction of the total variance in changes in glacier mass explained by the GCMs and the observed past air temperature and precipitation datasets (details in 2.8). The variances explained by the GCMs and the observed past air temperature and precipitation datasets were derived for six (two observed past air temperature and three observed past precipitation datasets); nine (three GCMs and three observed past precipitation datasets); and six (three GCMs and two observed past air temperature datasets) patterns.

Figure 4 indicates the fractional (relative) uncertainty in future glacier mass change caused by each input component (GCM, observed past air temperature, and observed past precipitation). The fractional uncertainty arising from the GCMs was around 60% at the beginning of the twenty-first century, and then increased slightly to become about 85% at the end of the century. The fractional uncertainty arising from observed past air temperature was about 35% at the beginning of the century but decreased to around 10% at the end of the century. This contributed the second largest proportion of the total uncertainty. The fractional uncertainty arising from observed past precipitation accounted for around 5–10% of all uncertainty throughout the century.

3.3 Resolving the components of future changes in glacier mass

We found that differences in observed past climatic datasets (air temperature and precipitation) propagated about

Table 8 The parameters of the glacier “HYOGA2” model

	Input observed past climate data	Median	Standard deviation
DDFsnow (mm °C ⁻¹ day ⁻¹)	CRU-APHRODITE	1.0	0.700
	ERA-Interim-APHRODITE	3.0	0.997
	CRU-Sakai	1.0	0.700
	ERA-Interim-Sakai	3.0	0.997
	CRU-MSWEP	1.0	0.700
	ERA-Interim-MSWEP	3.0	0.997
DDFice (mm °C ⁻¹ day ⁻¹)	CRU-APHRODITE	3.0	0.700
	ERA-Interim-APHRODITE	5.0	1.56
	CRU-Sakai	3.0	0.700
	ERA-Interim-Sakai	4.5	2.428
	CRU-MSWEP	3.0	0.700
	ERA-Interim-MSWEP	5.0	3.239
Cp (-)	CRU-APHRODITE	2.0	0.437
	ERA-Interim-APHRODITE	1.0	0.537
	CRU-MSWEP	2.0	0.412
	ERA-Interim-MSWEP	0.8	0.598
dT (°C)	CRU-APHRODITE	1.0	2.146
	ERA-Interim-APHRODITE	1.5	0.840
	CRU-Sakai	-0.375	0.951
	ERA-Interim-Sakai	1.0	0.367
	CRU-MSWEP	2.0	1.653
	ERA-Interim-MSWEP	1.875	0.466

The degree-day factors (DDFs) for ice and snow, and adjustment factors for precipitation (Cp) and temperature (dT) data, are shown

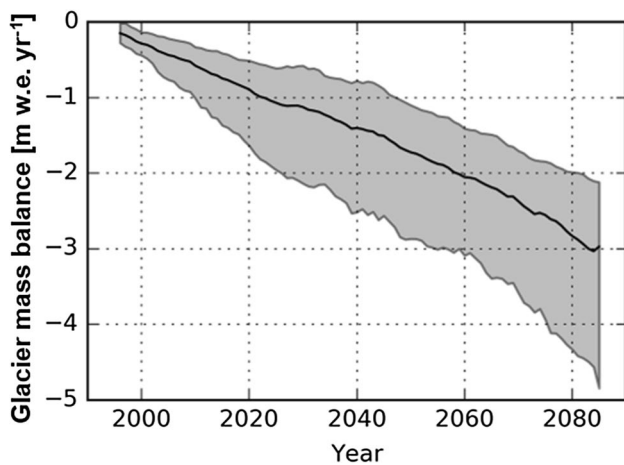


Fig. 3 Ensemble projections of future changes in glacier mass through 2100 using a set of 18 combinations of observed air temperature datasets, observed precipitation datasets, and GCMs; the 30 yr moving average of annual glacier changes through 2100 is shown for each simulation. Shading indicates the maximum and minimum range of the 18 simulations in each year. Thick lines indicate the mean of 18 simulations in each year

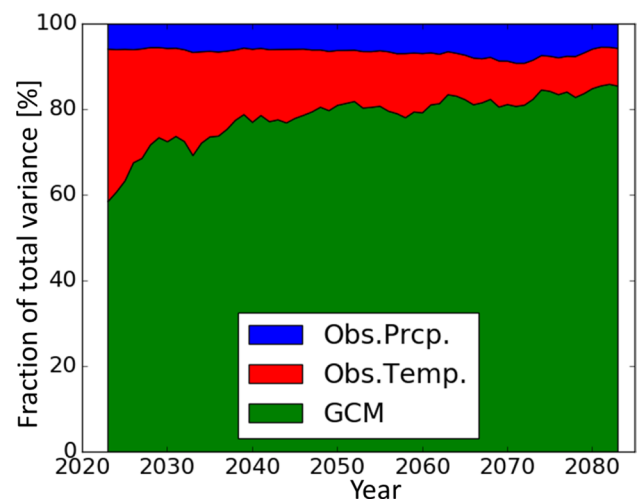


Fig. 4 Fraction of total variance in projections of changes in glacier mass explained by GCM, observed air temperature, and observed precipitation; 30 year moving average

5–35% fractional uncertainty throughout the twenty-first century (Sect. 3.2). To understand how observed past air temperature and precipitation data propagate uncertainties into future changes in glacier mass, three further analyses were conducted.

3.3.1 Observed past air temperature and precipitation for bias correction and glacier model calibration

The mean annual average air temperature and total precipitation, which were used for bias correction and model calibration, differed among the observed past climatic datasets (Tables 1, 2). In particular, the differences among observed past precipitation datasets were quite large, with the values from MSWEP being nearly double those of other datasets. The coefficient of variation for the observed past precipitation datasets was larger than that for the observed past air temperature datasets (Table 3).

3.3.2 Attribution of uncertainties in projected air temperature and precipitation

Projected future air temperature and precipitation were the only climatic factors driving future changes in modeled glacier mass. We partitioned the uncertainty components of projected future air temperature and precipitation after bias correction; we derived adjustment factors for precipitation (C_p) and air temperature (dT). Figure 5 shows the fractional (relative) uncertainties attributed to the GCM, observed past air temperature dataset, and observed past precipitation dataset for projected future air temperature (Fig. 5a) and precipitation (Fig. 5b). The uncertainties for both propagated from not only the different GCMs but also the differences in observed past climatic data used for bias correction and calibration. We confirmed that the past observed past

precipitation varied significantly among datasets (Tables 1, 2 and 3) and that differences in observed past precipitation were the dominant component of the uncertainty in projections of future precipitation (Fig. 5b).

3.3.3 Components of glacier mass budget

After determining future air temperature and precipitation employing bias correction and calibration, we used the model to calculate glacier ablation (mass loss) and glacier accumulation (mass gain), and derived a mass budget. Finally, the components of changes in glacier mass were resolved into ablation and accumulation (Fig. 6). Ablation

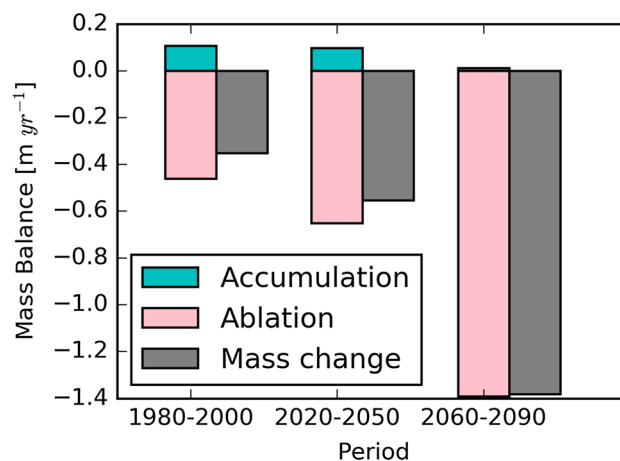


Fig. 6 Modeled components of the glacier mass budget. Bars show 20–30 year averages of accumulation (light blue), melt (pink), and mass change rates (gray) based on ERA-Interim observed past air temperatures, MSWEP observed past precipitation data, and future climate projections by MRI-CGCM3 (20-year average for 1980–2000, 30-year averages for 2020–2050 and 2060–2090)

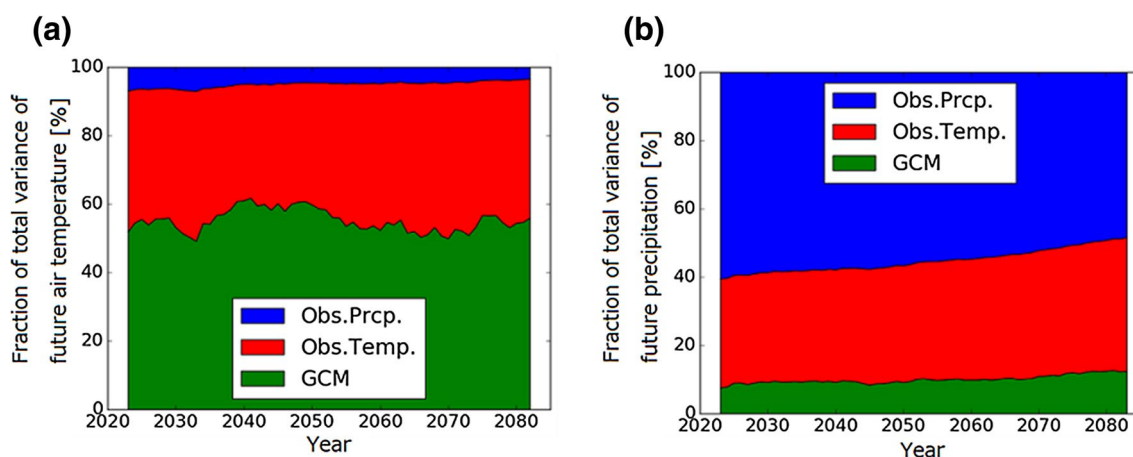


Fig. 5 Fraction of total variance in projections of air temperature (a) and precipitation (b) explained by the GCM, observed air temperature, and observed precipitation; 30 year moving average

was the mass loss yielding positive temperature sums in the model (details in Sect. 2.3). Accumulation was calculated as mass transferred from the snowpack above glaciers to glacier ice. The snowpack was calculated based on precipitated snow. We confirmed that the difference in observed past precipitation was the dominant fractional uncertainty in projections of future precipitation (Fig. 5b), but the accumulation, which was calculated based on future precipitation, was much smaller than the amount of ablation (Fig. 6). The impact of accumulation was very small compared to that of ablation; accumulation did not counter ablation.

4 Discussion

The uncertainty in projected changes in glacier mass was partitioned into three distinct sources: GCM uncertainty, observed past air temperature uncertainty, and observed past precipitation uncertainty. The fractions of uncertainty arising from the choice of past air temperature and precipitation datasets were about 15%, whereas that due to climate projections by the various GCMs was about 85% by the end of the century (Fig. 4). We confirmed that this result did not depend on the time period used to derive moving averages of uncertainty fractions (Supplement 3). Observed past precipitation differed significantly among datasets, and these differences propagated to become the dominant fraction of uncertainty in future precipitation projections (Tables 1, 2 and 3, Fig. 5b). However, the range of future precipitation was not the major uncertainty in projections of future changes in glacier mass (Fig. 4).

Previous global glacier model studies have often discussed the uncertainty in projecting future changes in glacier mass caused by the range of future air temperature and precipitation projections among GCMs (Giesen and Oerlemans 2013; Hirabayashi et al. 2013; Huss and Hock 2015; Radic et al. 2014), but none have considered the uncertainty caused by differences in climate datasets used for bias correction of GCMs and calibration of glacier models. Koppes et al. (2015) quantified the sensitivity of projections of glacier runoff to observed past air temperature datasets (past climatic forcings). The model parameters were held constant when using various observed past air temperature datasets; GCMs were not employed. We evaluated the uncertainties in projected mass changes caused by both observed past air temperatures and precipitation. Uncertainties arising from observed past climatic data are propagated not only by past climatic forcing but also by parameters of the glacier model and the GCM bias corrections. We are the first to identify the sources of uncertainty (Marzeion et al. 2012; Hirabayashi et al. 2013; Radic et al. 2014; Huss and Hock 2015; Koppes et al. 2015).

Ideally, there should be no differences in observed past climatic data. However, such differences propagated about

15% of the fractional uncertainty into projected future change in glacier mass by the end of the century. The remaining fractional uncertainty caused by GCM spread includes variabilities caused by each model's underlying theory and they would remain, although part of it can be reduced by the continuous efforts to improve GCMs. However, the fractional uncertainties arising from differences in observed past air temperatures and precipitation must be reduced. We found that use of some combinations of observed past climate datasets was relatively less biased when simulating past glacier mass balance using the HYOGA2 (Supplement 2). The combination may differ by the glacier model chosen. Further studies are necessary to evaluate observed past climate datasets when using them to compute changes in glacier mass using a method similar to that described in Massonnet et al. (2016). Additional studies to develop enhanced observed past climate datasets are also needed. State-of-the-art remote sensing satellites such as the Global Precipitation Measurement (GPM) Dual-Frequency Precipitation Radar (DPR) will reduce the differences among observed past climate datasets in regions with glaciers region. The GPM DPR seeks to measure both light and solid precipitation accurately and comprehensively. Modern rain gauges with windshields (e.g., the Geonor system) will be used to correct satellite observations, which may be unreliable if the topography is complex.

The impact of the differences among observed past precipitation datasets on projected changes in glacier mass was expected to be large due to the significant differences among the datasets. Although these differences caused a major fraction of the uncertainty in projected future precipitation, which was the dominant factor in calculating glacier accumulation, they did not trigger significant variation in the ultimate glacier mass change projection. This is because accumulation was not the dominant component of the glacier mass budget in this simulation. The use of a high-emissions scenario, the characteristics of the sampled glaciers, and the sensitivity of the temperature index glacier model to changing temperature may have resulted in less accumulation.

The results presented here refer to glaciers in the high mountains of Asia, and the uncertainties are not directly transferable to other study sites. Here, we assessed uncertainties in several past climatic datasets; we treated the gridded datasets as observational datasets. If local observation uncertainty could be directly assessed, it might be larger than we found; very few local data are available for glaciers. Additional uncertainties might arise from the choice of bias correction method or simplifications to the glacier model. The effects of model simplification are difficult to assess, as in most cases no alternative model exists. Therefore, future work should include multiple glacier models and should assess different glaciated regions, which could eventually lead to a comprehensive uncertainty assessment.

5 Conclusion

We projected mass changes in Asian glaciers through 2100 using a glacier model. We used a set of 18 combinations of two observed past air temperature datasets, three observed past precipitation datasets, and projected air temperatures and precipitations from three GCMs as inputs to assess the uncertainties arising from each component. The uncertainty was partitioned into three distinct sources: GCM uncertainty, observed past air temperature uncertainty, and observed past precipitation uncertainty. We found that the fractional uncertainties arising from the choice of observed past air temperature and precipitation datasets were about 15% by the end of the twenty-first century because of bias correction and parameter choice, although that due to climate projections by the various GCMs was dominant. The fractional uncertainties of observed past climatic datasets must be reduced. Differences in observed past climatic data affected estimates of future temperature and precipitation data input into the glacier model. However, these did not propagate equally into the major uncertainty in projection of glacier mass based on the mass budget. Differences among observed past precipitations were more significant than those among observed past air temperatures, but the fractional precipitation uncertainty was about 33–50% that of temperature when glacier ablation was dominant. This study suggests that glacier models should use multiple observed past climate datasets for bias correction and glacier model calibration for projection of future changes in glacier mass.

Acknowledgements This study received funding from Grant-in-Aid for Specially promoted Research (ID: 16H06291) and JSPS (Japan Society for Promotion of Science) Grant-in-Aid for Scientific Research (ID: 25008718). Thanks to A. Sakai for sharing data on precipitation published in Sakai et al. (2015).

Open Access This article is distributed under the terms of the Creative Commons Attribution 4.0 International License (<http://creativecommons.org/licenses/by/4.0/>), which permits unrestricted use, distribution, and reproduction in any medium, provided you give appropriate credit to the original author(s) and the source, provide a link to the Creative Commons license, and indicate if changes were made.

References

- Adam JC, Clark EA, Lettenmaier DP, Wood EF (2006) Correction of global precipitation products for orographic effects. *J Clim* 19:15–38. <https://doi.org/10.1175/jcli3604.1>
- Andermann C, Bonnet S, Gloaguen R (2011) Evaluation of precipitation data sets along the Himalayan front. *Geochem Geophys Geosyst*. <https://doi.org/10.1029/2011gc003513>
- Beck C, Grieser J, Rudolf B (2005) A new monthly precipitation climatology for the global land areas for the period 1951 to 2000. German Weather Service, Offenbach
- Beck HE, Van Dijk AIJM, Levizzani V et al (2017) MSWEP: 3-hourly 0.25° global gridded precipitation (1979–2015) by merging gauge, satellite, and reanalysis data. *Hydrol Earth Syst Sci* 21:589–615. <https://doi.org/10.5194/hess-21-589-2017>
- Biemans H, Hutjes RWA, Kabat P et al (2009) Effects of precipitation uncertainty on discharge calculations for Main River Basins. *J Hydrometeorol* 10:1011–1025. <https://doi.org/10.1175/2008jhm1067.1>
- Bliss A, Hock R, Radić V (2014) Global response of glacier runoff to twenty-first century climate change. *J Geophys Res Earth Surf*. <https://doi.org/10.1002/2013jfg002931>
- Bolch T, Kulkarni A, Kaab A et al (2012) The state and fate of Himalayan Glaciers. *Science*. <https://doi.org/10.1126/science.1215828>
- Bookhagen B, Strecker MR (2008) Orographic barriers, high-resolution TRMM rainfall, and relief variations along the eastern Andes. *Geophys Res Lett* 35:1–6. <https://doi.org/10.1029/2007gl032011>
- Brun F, Berthier E, Wagnon P et al (2017) A spatially resolved estimate of High Mountain Asia glacier mass balances from 2000 to 2016. *Nat Geosci*. <https://doi.org/10.1038/ngeo2999>
- Dahri ZH, Ludwig F, Moors E et al (2016) An appraisal of precipitation distribution in the high-altitude catchments of the Indus basin. *Sci Total Environ* 548–549:289–306. <https://doi.org/10.1016/j.scitotenv.2016.01.001>
- Dyrugerov MB (2010) Reanalysis of glacier changes: from the IGY to the IPY, 1960–2008. *Data Glaciol Stud* 108:1–116
- Dyrugerov MB, Meier MF (1997) mass balance of mountain and sub-polar glaciers: a new global assessment for 1961–1990. *Arct Alp Res* 29:379–391. <https://doi.org/10.2307/1551986>
- Dyrugerov MB, Meier MF (2005) Glaciers and the changing earth system: a 2004 snapshot. *Occas Pap* 58, Inst Arct Alp Res 15
- Global Energy and Water Exchanges (2013) GEWEX plans for 2013 and beyond. http://www.gewex.org/gewex-content/uploads/2015/02/GEWEX_Science_Questions_final.pdf. Accessed 20 Aug 2018
- Fujita K, Nuimura T (2011) Spatially heterogeneous wastage of Himalayan glaciers. *Proc Natl Acad Sci* 108:14011–14014. <https://doi.org/10.1073/pnas.1106242108>
- Fujita K, Sakai A, Takenaka S et al (2013) Potential flood volume of Himalayan glacial lakes. *Nat Hazards Earth Syst Sci* 13:1827–1839. <https://doi.org/10.5194/nhess-13-1827-2013>
- Gardner AS, Moholdt G, Cogley JG et al (2013) A reconciled estimate of glacier contributions to sea level rise: 2003 to 2009. *Science*. <https://doi.org/10.1126/science.1234532>
- Giesen RH, Oerlemans J (2013) Climate-model induced differences in the 21st century global and regional glacier contributions to sea-level rise. *Clim Dyn*. <https://doi.org/10.1007/s00382-013-1743-7>
- Hawkins E, Sutton R (2011) The potential to narrow uncertainty in projections of regional precipitation change. *Clim Dyn* 37:407–418. <https://doi.org/10.1007/s00382-010-0810-6>
- Hirabayashi Y, Kanae S, Motoya K et al (2008a) A 59-year (1948–2006) global meteorological forcing data set for land surface models. Part II: global snowfall estimation. *Hydrol Res Lett* 2:65–69. <https://doi.org/10.3178/hrl.2.65>
- Hirabayashi Y, Kanae S, Motoya K et al (2008b) A 59-year (1948–2006) global near-surface meteorological data set for land surface models. Part I: development of daily forcing and assessment of precipitation intensity. *Hydrol Res Lett* 2:36–40. <https://doi.org/10.3178/hrl.2.36>
- Hirabayashi Y, Zang Y, Watanabe S et al (2013) Projection of glacier mass changes under a high-emission climate scenario using the global glacier model HYOGA2. *Hydrol Res Lett* 7:6–11. <https://doi.org/10.3178/hrl.7.6>
- Huss M, Hock R (2015) A new model for global glacier change and sea-level rise. *Front Earth Sci*. <https://doi.org/10.3389/feart.2015.00054>

- Immerzeel WW, van Beek LPH, Bierkens MFP (2010) Climate change will affect the Asian water towers. *Science*. <https://doi.org/10.1126/science.1183188>
- Kääb A, Berthier E, Nuth C et al (2012) Contrasting patterns of early twenty-first-century glacier mass change in the Himalayas. *Nature* 488:495–498. <https://doi.org/10.1038/nature11324>
- Kaser G, Grosshauser M, Marzeion B (2010) Contribution potential of glaciers to water availability in different climate regimes. *Proc Natl Acad Sci*. <https://doi.org/10.1073/pnas.1008162107>
- Koppes M, Rupper S, Asay M, Winter-Billington A (2015) Sensitivity of glacier runoff projections to baseline climate data in the Indus River basin. *Front Earth Sci* 3:1–14. <https://doi.org/10.3389/feart.2015.00059>
- Lutz AF, Immerzeel WW, Shrestha AB, Bierkens MFP (2014) Consistent increase in High Asia's runoff due to increasing glacier melt and precipitation. *Nat Clim Change* 4:587–592. <https://doi.org/10.1038/nclimate2237>
- Marzeion B, Jarosch AH, Hofer M (2012) Past and future sea-level change from the surface mass balance of glaciers. *Cryosphere* 6:1295–1322. <https://doi.org/10.5194/tc-6-1295-2012>
- Marzeion B, Kaser G, Maussion F, Champollion N (2018) Limited influence of climate change mitigation on short-term glacier mass loss. *Nat Clim Change*. <https://doi.org/10.1038/s41558-018-0093-1>
- Massonnet F, Bellprat O, Guemas V, Doblus-Reyes FJ (2016) Using climate models to estimate the quality of global observational data sets. *Science* 354:452–455. <https://doi.org/10.1126/science.aaf6369>
- Palazzi E, Von Hardenberg J, Provenzale A (2012) Precipitation in the Karakorum and Himalaya from observations and global climate model simulations. Circulation patterns in the Hindu-Kush Karakoram Himalaya (HKKH) and the Indian Subcontinent. 13–15
- Parker WS (2016) Reanalyses and observations: what's the difference? *Bull Am Meteorol Soc* 97:1565–1572. <https://doi.org/10.1175/bams-d-14-00226.1>
- Radić V, Bliss A, Beedlow AC et al (2014) Regional and global projections of twenty-first century glacier mass changes in response to climate scenarios from global climate models. *Clim Dyn* 42:37–58. <https://doi.org/10.1007/s00382-013-1719-7>
- Sakai A, Fujita K (2017) Contrasting glacier responses to recent climate change in high-mountain Asia. *Sci Rep* 7:13717. <https://doi.org/10.1038/s41598-017-14256-5>
- Sakai A, Nuimura T, Fujita K et al (2015) Climate regime of Asian glaciers revealed by GAMDAM glacier inventory. *Cryosphere* 9:865–880. <https://doi.org/10.5194/tc-9-865-2015>
- Serreze MC, Walsh JE, Chapin FSI et al (2000) Observational evidence of recent change in the northern high-latitude environment. *Clim Change* 46:159–207. <https://doi.org/10.1023/a:1005504031923>
- Slangen ABA, Meysingnac B, Agosta C et al (2017) Evaluating model simulations of twentieth-century sea level rise. Part I: global mean sea level change. *J Clim* 30:8539–8563. <https://doi.org/10.1175/jcli-d-17-0110.1>
- Stocker TF (ed) (2014) *Climate change 2013: the physical science basis: working group I contribution to the fifth assessment report of the intergovernmental panel on climate change*. Cambridge University Press
- Wada Y, Wisser D, Eisner S et al (2013) Multimodel projections and uncertainties of irrigation water demand under climate change. *Geophys Res Lett* 40:4626–4632. <https://doi.org/10.1002/grl.50686>
- Watanabe S, Kanae S, Seto S et al (2012) Intercomparison of bias-correction methods for monthly temperature and precipitation simulated by multiple climate models. *J Geophys Res Atmos* 117:1–13. <https://doi.org/10.1029/2012jd018192>
- Watanabe M, Yanagawa A, Hirabayashi Y et al (2018) Uncertainty from climate forcing of projections in glacier melt for High Mountain Asia. *J Jpn Soc Civ Eng* 74:211–216
- Yatagai A, Kamiguchi K, Arakawa O et al (2012) Aphrodite constructing a long-term daily gridded precipitation dataset for Asia based on a dense network of rain gauges. *Bull Am Meteorol Soc* 93:1401–1415. <https://doi.org/10.1175/bams-d-11-00122.1>

Publisher's Note Springer Nature remains neutral with regard to jurisdictional claims in published maps and institutional affiliations.